Honeybee-inspired dynamics for multi-agent decision-making

Rebecca Gray Alessio Franci Vaibhav Srivastava Naomi Ehrich Leonard

Abstract

When choosing between nest sites, a honeybee swarm makes decisions that are sensitive to the values of the alternatives. Value-sensitivity is enabled by a distributed social effort among the honeybees, and it leads to decision-making dynamics of the swarm that are efficient, robust and adaptive. To explore and generalize these features to other networks, we design distributed multi-agent system dynamics that recover the high performing value-sensitive decision-making of the honeybees. Our framework uses tools of nonlinear dynamics to rigorously connect model-based investigation of the mechanisms of animal group decision-making dynamics more generally to systematic, bio-inspired design of coordinated control of multi-agent network systems. We augment the model by designing feedback dynamics for a bifurcation parameter to control system performance beyond that observed in swarms.

I. Introduction

For many applications of multi-agent systems, ranging from transportation networks and mobile sensing networks to power networks and synthetic biological networks, successful network-level decision-making among alternatives is fundamental to tasks that require coordination among agents. Enabling a group of individual agents to make a single choice among alternatives allows the group to collectively decide, for example, which alternative is true, which action to take, which direction or motion pattern to follow, or when something in the environment or in the state of the system has changed.

Since animals *rely* on collective decisions between alternatives for survival, we look to animal groups for inspiration. For example, a honeybee swarm makes a single, quick and accurate choice of the best quality nest site among scouted-out sites [1]. A fish school makes a single choice among potential food sources about which some individuals may have prior information or preference [2]. Migratory birds choose together when it is most

This research has been supported in part by NSF grant CMMI-1635056, ONR grant N00014-14-1-0635 and DGAPA-PAPIIT(UNAM) grant IA105816.

R. Gray and N. E. Leonard are with the Department of Mechanical and Aerospace Engineering, Princeton University, Princeton, NJ, USA, {rgray, naomi}@princeton.edu.

A. Franci is with the Department of Mathematics, Universidad Nacional Autónoma de México, Ciudad de México, Mexico, afranci@ciencias.unam.mx

V. Srivastava is with the Department of Electrical and Computer Engineering, Michigan State University, East Lansing, MI, USA, vaibhav@egr.msu.edu

efficient to depart a rest stop and continue on their route [3]. Indeed, from bird flocks to fish schools, animal groups are known to manage tasks, such as migration, foraging, and evasion, with speed, accuracy, robustness and adaptability [4], even though individuals employ distributed strategies with limitations on sensing, communication, and computation [5], [6].

As in the case of animal groups, successful operation of engineered networks in complex environments requires robustness to disturbance and adaptation in the face of changes in the environment. Further, like individual animals, agents in these kinds of networks typically use distributed control and have limitations on sensing, communication, and computation.

Mechanisms used to study collective animal behavior depend on the animals' social interactions and on their perceptions of their environment. A rigorous understanding of these dependencies makes possible the translation of the mechanisms into a systematic, bio-inspired design methodology for use in engineered networks. This remains a challenge, however, in part because most studies of collective animal behavior are empirically based or rely on mean-field models.

To address this challenge, we present a generalizable agent-based, dynamic model of distributed decision-making between two alternatives. In this type of decision-making, the pitchfork bifurcation is ubiquitous [7]; for example, it appears in the dynamics of honeybees choosing a nest site and schooling fish selecting a food source. Our approach is to derive the agent-based model so that it too exhibits the pitchfork bifurcation. This allows animal group dynamics and multi-agent dynamics to be connected mathematically by mapping to the normal form of the pitchfork bifurcation. The agent-based model provides an important complement to mean field or simulation models by allowing for rigorous analysis of the influence on system performance of distributed information, network topology, and other heterogeneities across the network.

Development of our framework has been largely influenced by the singularity theory approach to bifurcation problems [8]. The distinction among state, bifurcation, and the so-called unfolding parameters in that theory reflects the hierarchy among controlled variables, control variables, and tuning parameters in control theory. This analogy naturally translates bifurcation theory into control theory and guides the design of intrinsically nonlinear and tunable behaviors. This connection was originally made in [9] to design neuronal behaviors; see also [10] for a neuromorphic engineering application. In the present paper we prove results in cases with sufficient symmetry such that we do not require direct use of the tools of singularity theory. In future work we will exploit singularity theory [8] to extend results to the more general cases.

The generalizability of our framework provides a systematic way to translate a wide range of animal group dynamics into distributed multi-agent feedback dynamics; in this paper we focus the networked agent-based model dynamics on recovering the high performing, value-sensitive decision-making of a honeybee swarm choosing between two candidate nest sites as has been studied empirically and with a mean-field model [11], [12]; see [13] for an agent-based approach. Remarkably, honeybees efficiently and reliably select the highest value nest site, and for alternatives of equal value, they quickly make an arbitrary choice but only if the value is sufficiently high. Our framework also provides the means to study and design decision-making dynamics beyond that observed in

biological networks. To enhance control of network decision-making dynamics, we introduce a feedback law for a bifurcation parameter in the model. We prove stability using a time-scale separation of an all-to-all network and propose extensions to a general network topology and distributed external information. See related work on control of bifurcations [14], [15], [16].

The major contributions of our work are threefold. First, we introduce a generalizable agent-based, dynamic model for bio-inspired decision-making for a network of distributed agents. We use model reduction and asymptotic expansion to show how the model captures the adaptive and robust features of value-sensitive honeybee decision-making dynamics. Second, we investigate how the value of the alternatives, distribution of information, and interaction topology influence the decision-making dynamics in the agent-based model. Third, we show how to design slow feedback dynamics for a bifurcation parameter to enhance network decision-making.

In Section II, we present the agent-based decision-making model and prove a first theorem on the pitchfork bifurcation. Section III describes the honeybee decision-making dynamics, highlighting value-sensitive decision-making, adaptability and robustness. Model reduction to a low-dimensional, attractive manifold is proved in Section IV and used to prove an analytical approximation to the pitchfork bifurcation point. The theorems are used in Section V to show value-sensitivity, performance, and influence of model parameters in the agent-based model. In Section VI we present feedback dynamics of the bifurcation parameter and we conclude in Section VII.

II. Agent-based decision-making model

The proposed model is a specialization of the Hopfield network dynamics ([17], [18]). The model provides a generalizable network decision-making dynamic for a set of N interconnected agents and by design it exhibits a pitchfork bifurcation. To describe decision-making between two alternatives A and B, let $x_i \in \mathbb{R}$ be the state of agent i, representing its opinion, with $i \in \{1, ..., N\}$. Agent i is said to favor alternative A (B) if $x_i > 0$ (< 0), with the strength of agent i's opinion given by $|x_i|$. If $x_i = 0$, agent i is undecided. The collective opinion of the group is defined by $y(t) = \frac{1}{N}\sum_{i=1}^{N} x_i(t)$. Let y_{ss} and $\boldsymbol{x}_{\text{ss}}$ be steady state values of $y(t)$ and $\boldsymbol{x}(t) = (x_1, \ldots, x_N)^T$, respectively.

Let *disagreement* δ be defined by $\delta = |y_{\text{ss}}| - \frac{1}{N}\|\boldsymbol{x}_{\text{ss}}\|_1$, where $\|\cdot\|_1$ is the vector 1-norm. If each entry of $\boldsymbol{x}_{\text{ss}}$ has the same sign, then there is no disagreement, i.e, $\delta = 0$. We refer to the scenario with either $\boldsymbol{x}_{ss} = \mathbf{0}$ (no decision) or $\delta \neq 0$ (disagreement) as *deadlock*. A collective decision is made in favor of alternative A (resp. B) if $\delta = 0$ and $y_{\text{ss}} > \eta$ (resp. $y_{\text{ss}} < -\eta$), for some appropriately chosen threshold $\eta \in \mathbb{R}_{>0}$.

The network interconnections define which agents can measure the state of which other agents, and this is encoded using a network adjacency matrix $A \in \mathbb{R}^{N\times N}$. Each $a_{ij} \geq 0$ for $i, j \in \{1, ..., N\}$ and $i \neq j$ gives the weight that agent i puts on its measurement of agent j. Then $a_{ij} > 0$ implies that j is a neighbor of i. We let $a_{ii} = 0$ for all i and $D \in \mathbb{R}^{N\times N}$ be a diagonal matrix with diagonal entries $d_i = \sum_{j=1}^{N} a_{ij}$. $L = D - A$ is the Laplacian matrix of the graph associated with the interaction network.

We define the change in opinion of each agent over time as a function of the agent's current state, the state of

its neighbors and a possible external stimulus ν_i:

$$\frac{dx_i}{dt} = -u_1 d_i x_i + \sum_{j=1}^{N} u_2 a_{ij} S(x_j) + \nu_i. \tag{1}$$

$\nu_i \in \{\nu_{\mathrm{A}}, 0 - \nu_{\mathrm{B}}\}, \nu_{\mathrm{A}}, \nu_{\mathrm{B}} \in \mathbb{R}^+$ encodes the external information about an alternative received by agent i, or can represent the agent's preference among alternatives. If $\nu_i = \nu_{\mathrm{A}}$ (resp. $\nu_i = -\nu_{\mathrm{B}}$) agent i is informed about, or prefers, alternative A (resp. B). If $\nu_i = 0$ agent i receives no information or has no preference. $u_1 > 0$ and $u_2 > 0$ are control parameters and $S : \mathbb{R} \to \mathbb{R}$ is a smooth, odd sigmoidal function that satisfies the following conditions: $S'(z) > 0\ \forall z \in \mathbb{R}$ (monotone); $S(z)$ belongs to sector $(0, 1]$; and $\mathrm{sgn}(S''(z)) = -\mathrm{sgn}(z)$, where $(\cdot)'$ denotes the derivative with respect to the argument of the function, and $\mathrm{sgn}(\cdot)$ is the signum function.

The control u_1 can be interpreted as the *inertia* that prevents the agent from rapidly developing a strong opinion. The term $u_2 S(x)$ can be interpreted as the opinion of agent j as perceived by agent i. Since $S(x)$ is a saturating function, opinions of small magnitude are perceived as they are, while the perception of opinions of large magnitude will saturate at some cap. Control u_2 represents the strength of the *social effort*: a larger u_2 means a larger range of unsaturated perceived opinions.

Let $\boldsymbol{\nu} = (\nu_1, \ldots, \nu_N)^T$, and $\boldsymbol{S}(\boldsymbol{x}) = (S(x_1), \ldots, S(x_N))^T$. Then (1) can be written in vector form:

$$\frac{d\boldsymbol{x}}{dt} = -u_1 D\boldsymbol{x} + u_2 A\boldsymbol{S}(\boldsymbol{x}) + \boldsymbol{\nu}. \tag{2}$$

To simplify notation, we study (2) using a timescale change $s = u_1 t$. We denote $\boldsymbol{x}(s)$ by $\boldsymbol{x}$ and $d\boldsymbol{x}/ds$ by $\dot{\boldsymbol{x}}$. Let $u = u_2/u_1$, $\beta_i = \nu_i/u_1$, $\beta_{\mathrm{A}} = \nu_{\mathrm{A}}/u_1$, $\beta_{\mathrm{B}} = \nu_{\mathrm{B}}/u_1$ and $\boldsymbol{\beta} = (\beta_1, \ldots, \beta_N)^T$. Then each $\beta_i \in \{\beta_{\mathrm{A}}, 0, -\beta_{\mathrm{B}}\}$ and (2) is equivalent to

$$\dot{\boldsymbol{x}} = -D\boldsymbol{x} + uA\boldsymbol{S}(\boldsymbol{x}) + \boldsymbol{\beta}. \tag{3}$$

To see that these dynamics exhibit a pitchfork bifurcation, let the network graph be fixed, strongly connected, and balanced. Then $\mathrm{rank}(L) = N - 1$ and $\mathbf{1}_N^T L = L\mathbf{1}_N = \mathbf{0}$, where $\mathbf{1}_N$ is the vector of N ones. L has a zero eigenvalue with corresponding eigenvector $\boldsymbol{x} = \zeta\mathbf{1}_N$, $\zeta \in \mathbb{R}$, and every other eigenvalue has positive real part. Observe that the linearization of (3) at $\boldsymbol{x} = \mathbf{0}$ for $u = 1$ and $\boldsymbol{\beta} = \mathbf{0}$ is linear consensus dynamics $\dot{\boldsymbol{x}} = -L\boldsymbol{x}$, which converges to the consensus manifold $\boldsymbol{x} = \zeta\mathbf{1}_N$. This implies the possibility of a bifurcation with center manifold tangent to the one-dimensional consensus manifold [19, Theorem 3.2.1]. By odd symmetry of (1) for $\boldsymbol{\beta} = \mathbf{0}$, this will generically be a pitchfork [8, Theorem VI.5.1].

This is shown in Theorem 1 and illustrated Figure 1 for (3) specialized to an all-to-all network and $\boldsymbol{\beta} = \mathbf{0}$:

$$\dot{x}_i = -(N-1)x_i + \sum_{j \neq i}^{N} uS(x_j). \tag{4}$$

Theorem 1. *The following statements hold for the stability of invariant sets of dynamics* (4)*:*

(i) *The consensus manifold is globally exponentially stable for each* $u \in \mathbb{R} \geq 0$*;*

(ii) $\boldsymbol{x} = \mathbf{0}$ *is globally exponentially stable for* $u \in [0, 1)$ *and globally asymptotically stable for* $u = u^* := 1$*;*

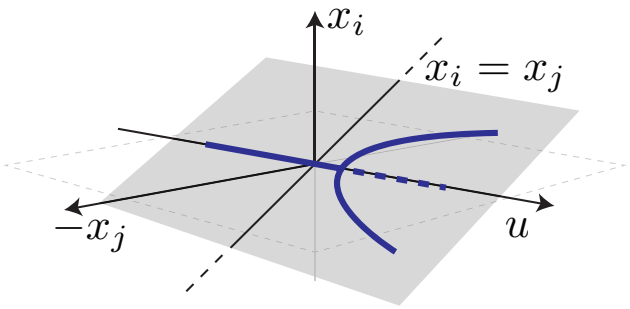

Fig. 1. For $u = 1$, dynamics (4) exhibit a pitchfork bifurcation at $\boldsymbol{x} = 0$. The steady-state branches emerging at the singularity lie on the consensus manifold $\{x_i = x_j | i, j \in \{1, ..., N\}\}$ shown in gray. Branches of stable and unstable solutions are shown as solid and dashed lines, respectively.

(iii) $\boldsymbol{x} = \mathbf{0}$ *is exponentially unstable and there exist two locally exponentially stable equilibrium points* $\pm\bar{y}(u)\mathbf{1}_N$ *for* $u > 1$*, where* $\bar{y}(u) > 0$ *is the positive non-zero solution of* $-y + uS(y) = 0$*. In particular, almost all trajectories converge to* $\pm\bar{y}(u)\mathbf{1}_N$ *for* $u > 1$*.*

Proof: Beginning with (i); consider a Lyapunov function $V_{ij}(\boldsymbol{x}) = \frac{(x_i - x_j)^2}{2}$. It follows that

$$\begin{aligned}\dot{V}_{ij}(\boldsymbol{x}) &= -(N-1)(x_i - x_j)(x_i - x_j + u(S(x_i) - S(x_j))) \\ &< -(N-1)(x_i - x_j)^2 = -2(N-1)V_{ij},\end{aligned}$$

for all $x_i \neq x_j$. Therefore, for $V(\boldsymbol{x}) = \sum_{i=1}^{n}\sum_{j=1}^{n} V_{ij}(\boldsymbol{x})$, $\dot{V}(\boldsymbol{x}) < -2(N-1)V(\boldsymbol{x})$, for all $\boldsymbol{x} \neq \zeta\mathbf{1}_N$, $\zeta \in \mathbb{R}$. $\dot{V}(\boldsymbol{x}) = 0$ for $x_i = x_j = \zeta$, so by LaSalle's invariance principle, the consensus manifold is globally exponentially stable.

Using (i), it suffices to study dynamics (4) on the consensus manifold, where they reduce to the scalar dynamics

$$\dot{y} = -(N-1)y + u(N-1)S(y).$$

(ii) and (iii) follow by inspection of these scalar dynamics and properties of S. ■

Remark 1 (Social effort breaks deadlock)**.** *Before the pitchfork (*$u < 1$*), the deadlock state* $\boldsymbol{x} = \mathbf{0}$ *is globally exponentially stable. After the pitchfork (*$u > 1$*), the deadlock state is unstable and two symmetric decision states are almost-globally asymptotically stable. Thus, our decision dynamics qualitatively capture a fundamental observation of social decision-making that increasing social effort breaks deadlock and leads to a decision through a pitchfork bifurcation.*

Remark 2 (Information with symmetry)**.** *The pitchfork remains for* $\boldsymbol{\beta} \neq \mathbf{0}$ *when the symmetry of the system is preserved, i.e., when* $\beta_A = -\beta_B$ *and the number of agents informed about A is equal to the number of agents informed about B. We prove this for a class of symmetric graphs in Theorem 3.*

Remark 3 (Asymmetry)**.** *The symmetry in* (3) *may be lost as a result of unequal values of the alternatives, unequal number of agents being exposed to each alternative, or the inherent asymmetry in the graph. The influence of asymmetry has been extensively studied in singularity theory using unfolding theory of "perturbed" bifurcations (see [8]). In particular, singularity theory establishes that as symmetry is lost the pitchfork bifurcation diagram generically unfolds into one of the four persistent bifurcation diagrams shown in Figure 2. Because the unfolding of the pitchfork is represented by a parametrized path in the unfolding of the cusp catastrophe [8, Section III.12], modulation of unfolding parameters (e.g., elements of* β*) is associated to a hysteresis phenomenon, which we show in Section V provides robustness in decision-making.*

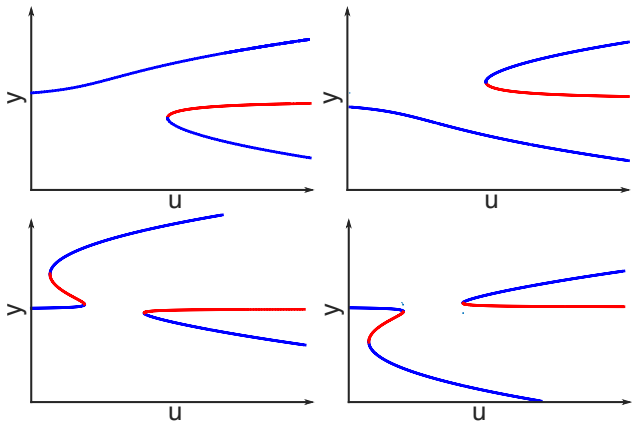

Fig. 2. Universal unfolding of the pitchfork: persistent bifurcation diagrams. Blue lines are stable solutions and red lines unstable solutions.

III. Honeybees and value-sensitive decision-making

When a honeybee swarm leaves an overpopulated nest, it must find a new high-value nest to survive the next winter and do so before the bees next need food. A small percentage of the swarm serve as scouts and these honeybees find and examine candidate nest sites, usually cavities in trees. The value of a candidate nest site is determined by features such as volume, size of entrance, and height above the ground. Remarkably, a honeybee swarm quickly and accurately chooses the highest value nest site among scouted-out sites [1]. Further, when candidate nest sites have near-equal value, honeybee swarms can still make highly efficient and robust choices [11]. Their decisions are sensitive both to the difference in value among the candidate nest sites and to the absolute values of the candidate nest sites [12]. This *value-sensitive decision-making* means that honeybee swarms can adapt their decisions to environmental changes in the value of available nest sites.

The mechanisms that explain the value-sensitive honeybee decision-making are rigorously studied in [12] using the model derived in [11]. Because the model represents a well-mixed (mean-field) population, it cannot directly be used to design distributed control strategies or to examine the influence of network topology or distribution of information across the group. However, since the analyses of [12] show that the mean-field model exhibits a

pitchfork bifurcation, we can design distributed agent-based dynamics that inherit the properties of the honeybee dynamics by connecting the mean-field dynamics to our generalizable agent-based model (3).

Once a honeybee has scouted out a candidate site, she uses explicit signaling in the form of a "waggle dance" on the vertical surface of the swarm to advertise and recruit uninformed bees to the site. A collective decision by the swarm for one site is made by a quorum. It was shown in [11] that, in addition to dancing to promote their discovered site, the scouts use a cross-inhibitory stop-signal to stop the dancing of the scouts recruiting for a competing site. This stop-signaling makes it possible for the swarm to make a quick (and random) decision in the case of two near-equal value sites, but to do so *only* if the nearly equal sites have sufficiently high value.

A model of the mean-field population-level dynamics of the swarm were derived in [11] under the assumption that the total bee population size N is very large. The model describes the dynamics of $y_A(t) = N_A(t)/N$ and $y_B(t) = N_B(t)/N$, the fraction of bees in the population committed to nest-site A and B at time t, respectively, and $y_U(t) = N_U/N$, the fraction of uncommitted bees in the population. Since $N = N_A + N_B + N_U$ is constant, $y_A + y_B + y_U = 1$ for all time t. Thus, the dynamics evolve on the two-dimensional unit simplex as

$$\begin{aligned}\frac{dy_{\mathrm{A}}}{dt} &= \gamma_{\mathrm{A}} y_U - y_{\mathrm{A}}(\alpha_{\mathrm{A}} - \rho_{\mathrm{A}} y_U + \sigma_{\mathrm{B}} y_{\mathrm{B}}) \\ \frac{dy_{\mathrm{B}}}{dt} &= \gamma_{\mathrm{B}} y_U - y_{\mathrm{B}}(\alpha_{\mathrm{B}} - \rho_{\mathrm{B}} y_U + \sigma_{\mathrm{A}} y_{\mathrm{A}}).\end{aligned} \tag{5}$$

γ_i is the rate of scout discovery and commitment, α_i the rate of abandonment, ρ_i the rate of recruitment and σ_i the rate of stop-signaling. It is assumed that $\gamma_i = \rho_i = \nu_i$ and $\alpha_i = \frac{1}{\nu_i}$ where ν_i is the assessed value of nest site i. Also, $\sigma_i = \sigma$, and so is equal for all sub-populations. A quorum decision is reached when y_A or y_B crosses threshold $\omega \in (0.5, 1]$.

For equal-value alternatives ($\nu_{\mathrm{A}} = \nu_{\mathrm{B}} = \nu$), there exists a critical rate of stop signaling $\sigma^* = \frac{4\nu^3}{(\nu^2-1)^2}$. If $\sigma < \sigma^*$ the system has one globally stable equilibrium at deadlock: $y_{\mathrm{A}} = y_{\mathrm{B}}$. For $\sigma > \sigma^*$ deadlock is unstable and there are two stable equilibria, each corresponding to a decision for one of the two alternatives. This is a pitchfork bifurcation with bifurcation parameter σ and bifurcation value $\sigma = \sigma^*$. The critical value σ^* is inversely dependent on the value ν of the alternatives, which allows the bees to adapt to their environment. Suppose that the bees use a fixed rate of stop-signaling σ. Then, when choosing between two low-valued alternatives they will remain in deadlock, presumably waiting for another nest site candidate to be discovered. But if the two equal alternatives are of high value, they will quickly choose one arbitrarily. Per Remark 1, for a given value ν, sufficiently large social effort σ yields a decision; for the honeybees, the required social effort for a decision increases with decreasing value of the alternatives.

Figure 3 shows the range of values ν and stop-signaling rate σ for which one solution (deadlock) and three solutions (two stable decisions and one unstable deadlock) exist, as well as the two-dimensional simplexes on which the dynamics evolve. The curve between regions describes the inverse relationship between the bifurcation point σ^* and the value ν.

If asymmetry $\nu_{\mathrm{A}} > \nu_{\mathrm{B}}$ is introduced in (5), the pitchfork bifurcation unfolds to yield a persistent bifurcation diagram as on the top left of Figure 2. The hysteresis associated with the perturbed pitchfork singularity provides

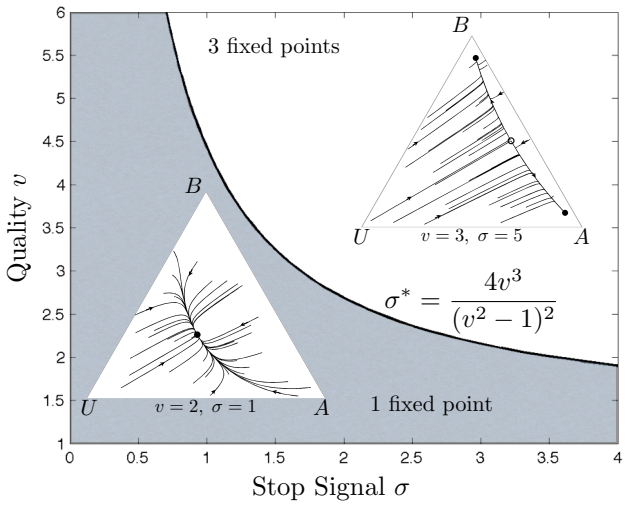

Fig. 3. From [12]. Value-sensitive decision-making for alternatives with equal value ν in mean-field model (5). The simplex on the left, representative of the grey area, shows convergence to the single stable equilibrium (black circle) at deadlock. The simplex on the right, representative of the white area, shows convergence to two stable equilibria at a decision for A or B. The curve that separates the region describes the inverse relationship of σ^* to ν.

robustness of the group decisions to small fluctuations in the relative value of the alternatives, with σ controlling what is meant by "small" [12]. If $\Delta\nu = \nu_{\mathrm{A}} - \nu_{\mathrm{B}} < 0$ and the decision has converged to B, then as $\Delta\nu$ increases, the solution does not switch to alternative A immediately as $\Delta\nu$ becomes positive but persists for small positive values of $\Delta\nu$ (and similarly for A and B swapped).

To explore these dynamics for equal alternatives in the agent-based model (Section V), set $u_1 = 1/\nu$ in (2) to get

$$\frac{d\boldsymbol{x}}{dt} = -\frac{1}{\nu}D(\boldsymbol{x}) + u_2 A\boldsymbol{S}(\boldsymbol{x}) + \boldsymbol{\nu}. \tag{6}$$

IV. Model reduction and bifurcation Analysis

Returning now to the agent-based model, for certain classes of network graph it is possible to identify a globally attractive, low-dimensional manifold on which to reduce the dynamics (3), and to perform analysis on the reduced model. The dimensionality N of the system is treated as a discrete parameter, allowing for the study of the sensitivity of the dynamics to the sizes of the informed and uninformed populations.

A. Model reduction to low-dimensional, attractive manifold

Let n_1 and n_2 be the number of agents with information $\beta_i = \beta_{\mathrm{A}} = \bar{\beta}_1$ and $\beta_i = -\beta_{\mathrm{B}} = \bar{\beta}_2$ respectively, and let $n_3 = N - n_1 - n_2$ be the number of agents with no information ($\beta_i = 0 = \bar{\beta}_3$). Let $\mathcal{I}_k \subset \{1, ..., N\}$, $k \in \{1, 2, 3\}$

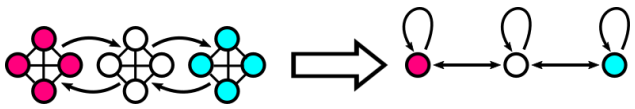

Fig. 4. Model reduction illustration. By Theorem 2 the graph (left) with $N = 12$ nodes, $n_1 = n_2 = n_3 = 4$ on (3) reduces to a three-dimensional system described by the graph (right) on (8). Pink agents have $\beta_i = 1$, white agents $\beta_i = 0$ and cyan agents $\beta_i = -1$. The self loops in the reduced model represent the influence of the others in the same group.

be the index set associated with each group. Also assume

$$a_{ij} = \begin{cases} \bar{a}_{km}, & \text{if } i \in \mathcal{I}_k,\ j \in \mathcal{I}_m, \text{ and } i \neq j \\ 0, & \text{otherwise} \end{cases},$$

for $i, j \in \{1, ..., N\}$, where $\bar{a}_{km} = 1$ if $k = m$. Under these assumptions, each node in the same group k has the same in-degree, $\bar{d}_k$, and opinion dynamics (3) for agent $i \in \mathcal{I}_k$ are

$$\dot{x}_i = -\bar{d}_k x_i + u \sum_{j \in \mathcal{I}_k} S(x_j) + u \sum_{\substack{m \in \{1,2,3\} \\ m \neq k}} \sum_{j \in \mathcal{I}_m} \bar{a}_{km} S(x_j) + \bar{\beta}_k. \tag{7}$$

Theorem 2 allows the analysis of (7) to be restricted to the subspace where each agent in the same group has the same opinion. The theorem is illustrated in Figure 4.

Theorem 2. *Every trajectory of the opinion dynamics* (7) *converges exponentially to the three-dimensional manifold*

$$\mathcal{E} = \{\boldsymbol{x} \in \mathbb{R}^N | x_i = x_j,\ \forall i, j \in \mathcal{I}_k, k = 1, 2, 3\}.$$

The dynamics on $\mathcal{E}$ *are*

$$\begin{aligned} \dot{y}_1 &= -\bar{d}_1 y_1 + u\big((n_1 - 1)S(y_1) + n_2 \bar{a}_{12} S(y_2) \\ &\qquad . + n_3 \bar{a}_{13} S(y_3)\big) - \beta_{\mathrm{A}} \\ \dot{y}_2 &= -\bar{d}_2 y_2 + u\big((n_2 - 1)S(y_2) + n_1 \bar{a}_{21} S(y_1) \\ &\qquad + n_3 \bar{a}_{23} S(y_3)\big) + \beta_{\mathrm{B}} \\ \dot{y}_3 &= -\bar{d}_3 y_3 + u\big((n_3 - 1)S(y_3) + n_1 \bar{a}_{31} S(y_1) \\ &\qquad + n_2 \bar{a}_{32} S(y_2)\big). \end{aligned} \tag{8}$$

Proof: Let $V(\boldsymbol{x}) = \sum_{k=1}^{3} V_k(\boldsymbol{x})$, where $V_k(\boldsymbol{x}) = \frac{1}{2} \sum_{i \in \mathcal{I}_k} \sum_{j \in \mathcal{I}_k} (x_i - x_j)^2,$ for $k \in \{1, 2, 3\}$. It follows that

$$\begin{aligned} \dot{V}_k(\boldsymbol{x}) &= \sum_{i \in \mathcal{I}_k} \sum_{j \in \mathcal{I}_k} (x_i - x_j)(\dot{x}_i - \dot{x}_j) \\ &= \sum_{i \in \mathcal{I}_k} \sum_{j \in \mathcal{I}_k} \big(-\bar{d}_k (x_i - x_j)^2 - u(x_i - x_j)(S(x_i) - S(x_j))\big) \\ &\leq -\bar{d}_k V_k(\boldsymbol{x}), \end{aligned}$$

so $\dot{V}(\boldsymbol{x}) \leq -\bar{d}_k V(\boldsymbol{x})$. By LaSalle's invariance principle, every trajectory of (7) converges exponentially to the largest invariant set in $V(\boldsymbol{x}) = 0$, which is $\mathcal{E}$. Let $y_k = x_i$, for any $i \in \mathcal{I}_k,\ k \in \{1,2,3\}$. Then dynamics (7) reduce to (8). ■

B. Pitchfork bifurcations in Z_2 symmetric, all-to-all networks

A vector field $F : \mathbb{R}^N \to \mathbb{R}^N$ is Z_2-symmetric when it commutes with the linear transformation

$$\gamma = \begin{bmatrix} 0_{n\times n} & -I_n & 0_{n\times(N-2n)} \\ -I_n & 0_{n\times n} & 0_{n\times(N-2n)} \\ 0_{(N-2n)\times n} & 0_{(N-2n)\times n} & -I_{N-2n} \end{bmatrix},$$

for $0 \leq 2n < N$. The dynamics (3) are Z_2-symmetric if $\beta_A = -\beta_B = \beta$, $n_1 = n_2 = n$, and the graph is symmetric. The class of graph discussed in Section IV-A is symmetric if $\bar{a}_{km} = \bar{a}_{mk}$, for each $k, m \in \{1,2,3\}$, and $\bar{a}_{13} = \bar{a}_{23}$. For this class Z_2 symmetry means that reversing the sign of β_A and β_B is equivalent to applying the transformation $\boldsymbol{x} \mapsto -\boldsymbol{x}$.

Consider an all-to-all graph with unit weights and $\beta_A = -\beta_B = \beta$, $n_1 = n_2 = n$, which make the dynamics (3) Z_2-symmetric. We can find an approximation $\hat{u}^*$ to the bifurcation point u^* by examining the reduced dynamics (8), which specialize to

$$\begin{aligned} \dot{y}_1 &= -(N-1)y_1 + u\big((n-1)S(y_1) \\ &\qquad + nS(y_2) + n_3 S(y_3)\big) + \beta \\ \dot{y}_2 &= -(N-1)y_2 + u\big(nS(y_1) \\ &\qquad + (n-1)S(y_2) + n_3 S(y_3)\big) - \beta \\ \dot{y}_3 &= -(N-1)y_3 + u\big(nS(y_1) \\ &\qquad + nS(y_2) + (n_3-1)S(y_3)\big). \end{aligned} \tag{9}$$

Because of Z_2 symmetry, the deadlock state $\boldsymbol{y}^*(u,\beta) = (y^*(u,\beta), -y^*(u,\beta), 0)$ is always an equilibrium, where $y^*(u,\beta)$ is the solution to

$$(N-1)y^* + uS(y^*) - \beta = 0. \tag{10}$$

When $\beta = 0$, $y^*(u,0) = 0$ for all $u \in \mathbb{R}$. When $\beta \neq 0$, the implicit function theorem ensures that $y^*(u,\beta)$ depends smoothly on u and β. By Taylor expansion, an approximation to $\boldsymbol{y}^*(u,\beta)$ can be found, and the bifurcation point where deadlock becomes unstable can also be approximated. To compare theoretical and numerical results, we let $S(\cdot) = \tanh(\cdot)$ in Theorem 3 but the computations are general.

Theorem 3. *For dynamics* (9) *with* $S(\cdot) = \tanh(\cdot)$*, the following statements hold:*

(i) *the equilibrium* $\boldsymbol{y}^*(u,\beta) = (y^*(u,\beta), -y^*(u,\beta), 0)$ *satisfies*

$$y^*(u,\beta) = \frac{1}{N-1+u}\beta + \frac{u}{3(N-1+u)^4}\beta^3 + \mathcal{O}(\beta^5); \tag{11}$$

(ii) *the equilibrium* $\boldsymbol{y}^* = (y^*, -y^*, 0)$ *is singular for*

$$u^* = 1 + \frac{(1+3N^3)^2(N-n_U)}{9n^9}\beta^2 + \mathcal{O}(\beta^4); \tag{12}$$

(iii) *for sufficiently small* β*, the singular equilibrium at* $u = u^*$ *is a pitchfork bifurcation.*

Proof: We begin with (i). Consider Taylor series expansion of $y^*(u,\beta)$:

$$y^*(u,\beta) = \beta y_1 + \beta^2 y_2 + \beta^3 y_3 + \beta^4 y_4 + \mathcal{O}(\beta^5). \tag{13}$$

Substitute $y^*(u,\beta)$ into (10) and differentiate with respect to β to get

$$(N-1)y^{*\prime}(u,\beta) + u\text{sech}^2\big(y^*(u,\beta)\big)y^{*\prime}(u,\beta) - 1 = 0.$$

Substituting in $\beta = 0$ yields $y_1 = \frac{1}{N-1+u}$. Proceeding similarly for higher order derivatives gives $y_2 = y_4 = 0$ and

$$y_3 = \frac{u}{3(N-1+u)^4}.$$

Substituting these values in (13) yields (11), establishing (i).

At a singular point u^*, the Jacobian of (9) computed at $\boldsymbol{y}^*$ drops rank. The Jacobian of (9) at $\boldsymbol{y}^*$ is

$$\begin{bmatrix} -(N-1)+u(n-1)S'(y^*) & unS'(y^*) & un_3 \\ unS'(y^*) & -(N-1)+u(n-1)S'(y^*) & un_3 \\ unS'(y^*) & unS'(y^*) & -(N-1)+u(n_3-1) \end{bmatrix},$$

where we have used the fact that $S'(\cdot)$ is an even function. For $S(\cdot) = \tanh(\cdot)$ the determinant d of the Jacobian is

$$d = -\frac{1}{4}\eta(-1+N+2u+\eta\text{cosh}(2y_1))(\eta+3u+n_3u-2Nu \\ -2u^2+(\eta+u-n_3u)\text{cosh}(2y_1))\text{sech}^4(y_1),$$

with $\eta = N-1$. A positive $u = u^*$ for which $d = 0$ satisfies

$$u^* = \frac{1}{4}(3+n_3-2N+\text{cosh}(2y^*)-n_3\text{cosh}(2y^* \\ +\sqrt{16\eta\text{cosh}^2(y^*)+(3+n_3-2N-(-1+n_3)\text{cosh}^2(2y^*]))}).$$

Note that y^* is also a function of u^* and the above equation is a transcendental equation in u^* that can be solved numerically. Here, we compute a Taylor series approximation to u^*. We know that for $\beta = 0$, $y^* = 0$ and $u^* = 1$. As above, we begin with the Taylor Series expansion $u^*(\beta) = 1 + u_1^*\beta + u_2^*\beta^2 + u_3^*\beta^3 + O(\beta^4)$ and match coefficients to obtain (12).

To prove that the singular point corresponds to a pitchfork we invoke singularity theory for Z_2-symmetric bifurcation problems [8, Chapter VI]. By Theorem 1, this singular point is a pitchfork for $\beta = 0$. Because (9) is Z_2 symmetric, for sufficiently small β we obtain a small Z_2-symmetric perturbation of the pitchfork for $\beta = 0$. Invoking genericity of the pitchfork in Z_2-symmetric systems [8, Theorem VI.5.1], we conclude that (9) possesses a pitchfork at $u = u^*$. ■

Remark 4 (Deadlock breaking)**.** *Theorem 3 shows persistence of the Theorem 1 bifurcation under* Z_2 *symmetry and weakly informed agents (*β *small). For small social effort (*$u < u^*$*) deadlock is the only stable equilibrium*

despite the presence of informed agents, but for sufficiently large social effort ($u > u^*$) deadlock is unstable. In the case of $\beta \neq 0$ an unstable deadlock state does not imply that deadlock has been broken, because differences in opinions can maintain disagreement for moderate social effort. The feedback control dynamics introduced in Section VI overcomes this by increasing the social effort beyond the destabilizing of deadlock.

Remark 5 (Influence of system parameters)**.** *The approximation* (12) *of u^* depends on value β, total group size N and uninformed group size n_3; it thus explicitly describes the sensitivity of the bifurcation to group size and information strength and distribution. We exploit this in Section V-B.*

V. Value-sensitivity and influence of system parameters in agent-based model

In this section we show how the agent-based dynamics (6) provide a multi-agent network system with the value-sensitivity and performance of the honeybees studied with the mean-field model (5). We use the agent-based model to examine the influence of system parameters, including size of the group and strength and distribution of information.

A. Value-sensitivity and performance in agent-based model

To show value-sensitivity and the associated robustness and adaptability in the agent-based model, we examine the dynamics (6) with bifurcation parameter $u_2 = u \cdot u_1 = \frac{u}{\nu}$. Applying the approximation (12) for u^* gives the approximation to the bifurcation point u_2^* for (6) as

$$\hat{u}_2^* = \frac{1}{\nu} + \frac{(1+3N^3)^2(N-n_U)}{9N^9}\nu^3 + \mathcal{O}(\nu^7). \tag{14}$$

Figure 5 shows how well $\hat{u}_2^*$ approximates u_2^* computed using MatCont continuation software [20]. As in the case of the honeybee mean-field model (see Figure 3), the bifurcation point in the agent-based model depends inversely on the value of the alternatives ν (see (14) and Figure 5). Thus, our agent-based decision-making model recovers the value-sensitive decision-making of the honeybee mean-field model.

This value-sensitivity is demonstrated further in Figure 6, where bifurcation diagrams for the agent-based model are given for a range of values ν. As ν is increased, the bifurcation point decreases and the sharpness of the bifurcation branches increases, representing a faster increase in average opinion.

The value-sensitivity of the agent-based dynamics implies the adaptability of the network to the environment as seen in the mean field model; that is, in the case of equal-value alternatives, the multi-agent network will make a quick and random decision for one of the two alternatives but only if the value is sufficiently large. Further, because the agent-based model maps to the same pitchfork normal form as the mean-field model, the agent-based model implies the robustness to small changes in the difference in values of the alternatives discussed for the mean-field model in Section III. Figure 7 illustrates the hysteresis phenomenon that provides this robustness for the agent-based dynamics. Suppose $\nu_A > \nu_B$, the network has decided for A, but ν_{A} decreases. The group will resist changing its decision to B unless ν_{A} is sufficiently less than ν_{B} (unless $\Delta\nu < -1.2$ in Figure 7).

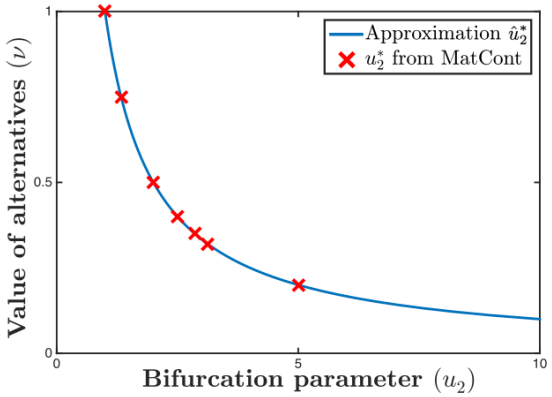

Fig. 5. Value-sensitive decision-making for alternatives with equal value ν in agent-based model (6). The curve shows how u_2^* depends inversely on ν, recovering the value sensitivity of the honeybee mean-field model (5); compare with Figure 3. The blue line shows the approximation u_2^* (14) while the red crosses show u_2^* computed numerically using continuation software. Informed and uninformed group sizes are $n_1 = n_2 = n = 10$ and $n_3 = 80$.

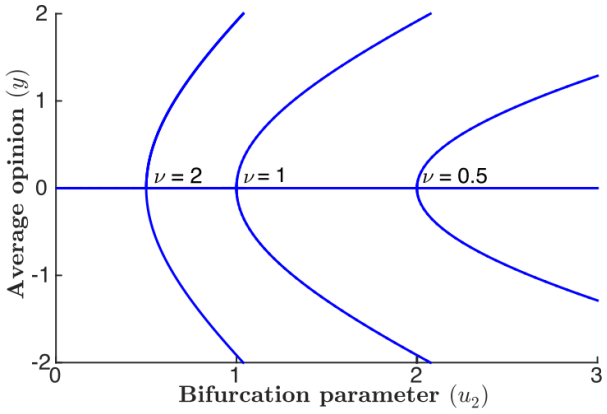

Fig. 6. Bifurcation diagrams for agent-based model (6) with $n_1 = n_2 = 10$, $n_3 = 80$ and three values of ν.

B. Influence of system parameters in agent-based model

An advantage of the agent-based framework is that it makes it possible to systematically study sensitivity of the dynamics to model parameters including those that describe network structure and heterogeneity. An examination of (14) shows that $\hat{u}_2^*$ decreases with increasing total group size N, implying that less social effort is required to make a decision with a larger group. In the limit as N increases, $\hat{u}_2^* = \frac{1}{\nu}$.

Figure 8 shows the inverse relationship between ν and $\hat{u}_2^*$ for different values of n_3 with fixed N and $n_1 = n_2 = N - 2n_3$. As n_3 increases, the number of informed agents decreases, and the curve drops implying that increasing the number of uninformed agents reduces the requirement on social effort to destabilize deadlock. This result suggests that the agent-based dynamics could be mapped to describe the schooling fish decision dynamics

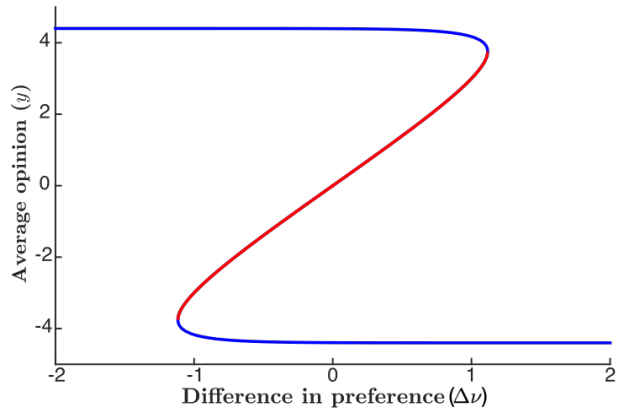

Fig. 7. Hysteresis associated with varying $\Delta\nu = \nu_{\rm A} - \nu_{\rm B}$ in the agent-based model. This gives rises to robustness with respect variation in values. The plot shows stable (blue) and unstable (red) solutions y as a function of Δv for $u_2 = 1.1$, $n_1 = n_2 = 3$, $n_3 = 4$, and $(\nu_{\rm A} + \nu_{\rm B})/2 = 10$.

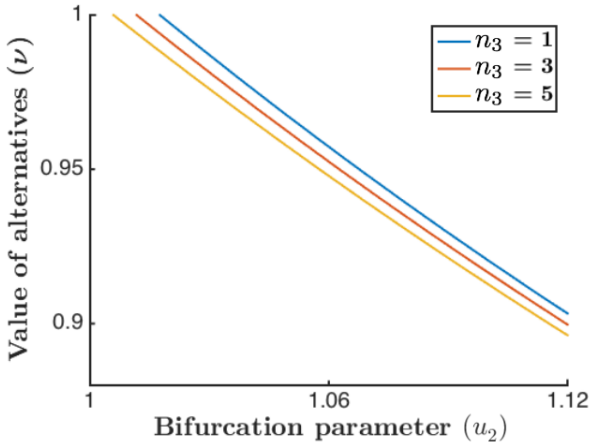

Fig. 8. The inverse relationship between ν and $\hat{u}_2^*$ from (14) in the agent-based model for three values of n_3 with $N = 7$ and $n_1 = n_2 = N - 2n_3$.

discussed in [2], where it is shown that increasing the number of uninformed agents allows the group to choose the alternative preferred by the majority over a more strongly influencing but minority preference.

Formal proofs of the influence of parameters in the absence of Z_2 symmetry will be described in future work. Here, we numerically investigate (3) for generic balanced connected graphs and asymmetric value of alternatives ($\nu_{\rm A} \neq \nu_{\rm B}$). When no information is present in the network ($\boldsymbol{\beta} = \mathbf{0}$), the system is Z_2-symmetric for a generic balanced graph and exhibits a symmetric pitchfork bifurcation. However, in the presence of information ($\boldsymbol{\beta} \neq \mathbf{0}$) the symmetric pitchfork breaks according to the pitchfork unfolding in Figure 2. For small u the group choice for the larger value alternative is the sole stable attractor and only for sufficiently large u does the attractor corresponding to

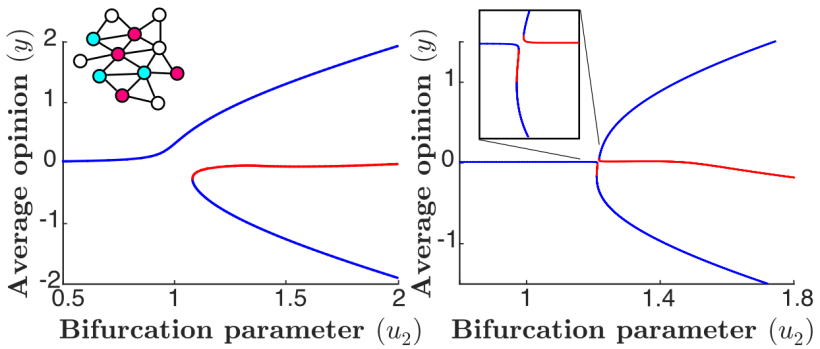

Fig. 9. Left: perturbation of pitchfork for balanced graph with heterogeneous information. Right: a qualitatively different perturbation of the pitchfork.

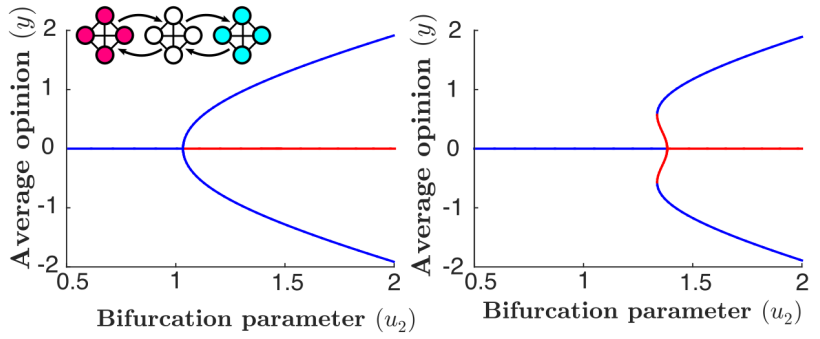

Fig. 10. Left: sharpening of the pitchfork with $\beta = 1$. Right: subcritical pitchfork in a Z_2-symmetric graph with $\beta = 3$.

the group choice for the smaller value alternative appear in a fold (saddle node) bifurcation (Figure 9 left). Another perturbation of the symmetric pitchfork is possible, depending on opinions, in which the attractor corresponding to the group with larger value information appears in a fold bifurcation *before* deadlock is broken (Figure 9 right). In this case there is bistability between deadlock and the decision for the larger value alternative. For sufficiently large u the attractor associated to the choice for the smaller value alternative appears in a second fold bifurcation.

Figure 10 shows the bifurcation diagrams in the Z_2-symmetric network shown (also Figure 4). For small β we naturally find the Z_2-symmetric pitchfork. Increasing the information value leads to a "sharpening" of the pitchfork: the parabola of stable decision states becomes wider, which corresponds to faster increase of the average opinion, once deadlock is broken (Figure 10 left). Further increasing the information value leads to a subcritical pitchfork, in which the two stable decision branches appear *before* deadlock is broken (Figure 10 right). In this case, the network jumps to a large positive or negative average opinion once deadlock is broken, instead of slowly increasing or decreasing along one of the two stable branches. Phenomenologically, this is associated to a faster and more robust decision-making process.

VI. Feedback control of bifurcation

Given system parameters, including value of alternatives and number of agents, the bifurcation parameter u in (3) (u_2 in (6)) controls if and how a group decision is made. In this section we design slow feedback dynamics for u to enhance the decision-making of the multi-agent system. In Section VI-A we prove feedback dynamics for u in an all-to-all network that ensures a fast, arbitrary group decision in the case of equal value alternatives. In Section VI-B we propose dynamics that apply for a general network graph.

A. Control of bifurcation with all-to-all network graph

We consider the following feedback dynamics on the social effort u for the all-to-all system with N uninformed agents

$$\begin{aligned} \dot{\boldsymbol{x}} &= -D\boldsymbol{x} + uAS(\boldsymbol{x}), \\ \dot{u} &= \epsilon \left(y_{th}^2 - \left(\frac{1}{N} \mathbf{1}_N^T \boldsymbol{x} \right)^2 \right), \end{aligned} \tag{15}$$

where $0 < \epsilon < 1$. These dynamics augment the agent-based model (3) such that the social effort slowly increases until the magnitude of the average opinion $|y| > y_{th}$, where $y_{th} > 0$ is a desired threshold, e.g., as required for a quorum decision.

By virtue of Theorem 1(i) we can reduce the analysis of (15) to the consensus manifold $\boldsymbol{x} = \mathbf{1}_N y$. Then the closed-loop dynamics of the average opinion y satisfy

$$\begin{aligned} \dot{y} &= f(y,u) := (N-1)\big(-y + uS(y) \big), \\ \dot{u} &= g(y) := \epsilon \left(y_{th}^2 - y^2 \right) =: g(y). \end{aligned} \tag{16}$$

Behavior of equation (16) can be analyzed using singular perturbation theory [21], [22]. We define the slow time $\tau = \epsilon s$, which transforms (16) into the equivalent dynamics

$$\begin{aligned} \epsilon y' &= (N-1)\big(-y + uS(y) \big), \\ u' &= \left(y_{th}^2 - y^2 \right), \end{aligned} \tag{17}$$

where $' = \frac{d}{d\tau}$. For $\epsilon \ll 1$, (16) describe the *boundary layer* dynamics, evolving in fast time s:

$$\begin{aligned} \dot{y} &= (N-1)\big(-y + uS(y) \big), \\ \dot{u} &= 0, \end{aligned} \tag{18}$$

(17) describe the *reduced* dynamics, evolving in slow time τ:

$$\begin{aligned} 0 &= (N-1)\big(-y + uS(y) \big), \\ u' &= \left(y_{th}^2 - y^2 \right), \end{aligned} \tag{19}$$

defined on the *critical manifold* $M_0 = \{(y,u) : -y + uS(y) = 0\}$. Equilibria on M_0 are also equilibria of the boundary layer dynamics. Singular perturbation theory provides a qualitative picture of trajectories of the original

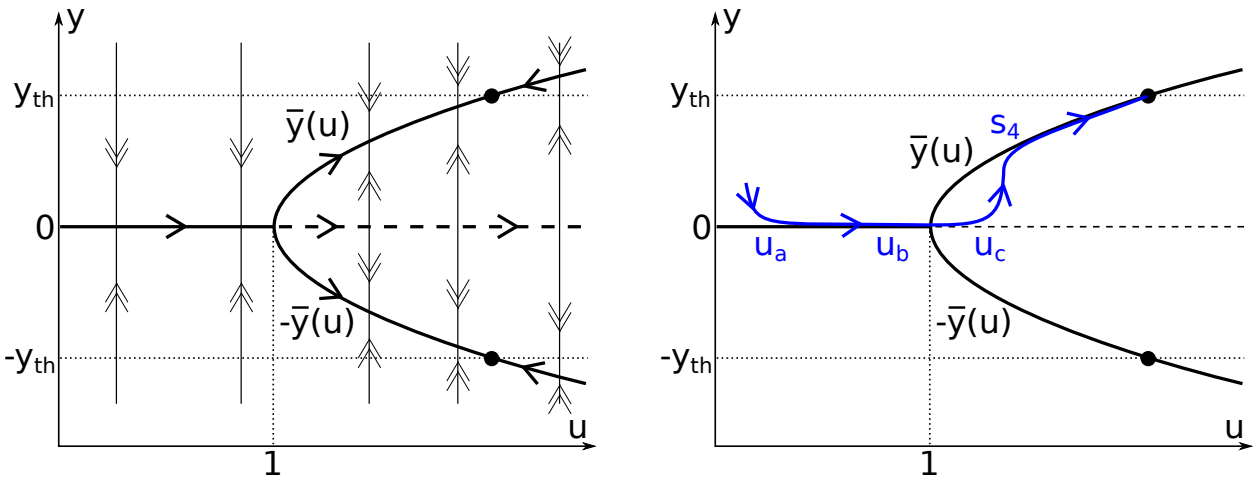

Fig. 11. Singular phase portrait (left) and typical trajectory (right) of the closed-loop dynamics (16)

dynamics: trajectories of the boundary layer dynamics are a good approximation of the original dynamics far from M_0, whereas trajectories of the reduced dynamics are a good approximation close to M_0.

Trajectories of the boundary layer and reduced dynamics are sketched in Figure 11 left. By Theorem 1 M_0 is composed of a single globally exponentially stable branch $y = 0$ for $u < 1$ and three branches emerging from a pitchfork bifurcation for $u > 1$. The outer branches $y = \pm\bar{y}(u)$ are locally exponentially stable and $y = 0$ is unstable. For a given u, trajectories of the boundary layer dynamics (double arrows) converge toward stable branches of M_0 and are repelled by unstable branches. On M_0, trajectories of the reduced dynamics (single arrow) satisfy $u' > 0$ if $|y| < y_{th}$ and $u' < 0$ if $|y| > y_{th}$.

Theorem 4 summarizes the qualitative behavior of the closed-loop dynamics for sufficiently small ϵ and $u(0) < 1$. The result is illustrated in Figure 11 right.

Theorem 4. *For all $y_{th} > 0$ and all $0 < u(0) < 1$, there exist $\bar{\epsilon} > 0$ and $0 < \delta < y_{th}$ such that, if $0 < \epsilon < \bar{\epsilon}$ and $|y(0)| < \delta$ the following hold:*

- *If $y(0) = 0$, then $y(s) = 0$ for all $s \geq 0$ and $u(s) \to \infty$ as $s \to \infty$.*
- *If $y(0) > 0$ (resp. $y(0) < 0$), there exist*

$$u_a = u(0) + \mathcal{O}(\epsilon|\log(\epsilon)|) \tag{20a}$$

$$u_b \geq u_a,\ 1 - \delta < u_b < 1 \tag{20b}$$

$$u_c = 2 - u_b - \mathcal{O}(\epsilon|\log(\epsilon)|) \tag{20c}$$

such that $\dot{u}(s) > 0$ for all s such that $u(0) \leq u(s) \leq u_c$ and $0 < y(s) \leq \epsilon$ (resp. $-\epsilon < y(s) < 0$) for all s such that $u_a \leq u(s) \leq u_c$. Let $s_3 = \operatorname{argmin}_s\{u(s) = u_c\}$. There exist $s_4 = s_3 + \mathcal{O}(\epsilon|\log(\epsilon)|)$ and $c_1 > 0$ such that $|y(s) - \bar{y}(u(s))| < c_1\epsilon$ (resp. $|y(s) + \bar{y}(u(s))| < c_1\epsilon$) for all $s \geq s_4$. Finally $y(s) \to y_{th}$ (resp. $y(s) \to -y_{th}$) and $u(s) \to \bar{y}^{-1}(y_{th})$ as $s \to \infty$.

Proof: The case $y(0) = 0$ is trivial as $\dot{y} \equiv 0$ and $\dot{u} \equiv \epsilon y_{th}^2$.

The case $y(0) \neq 0$ involves singular perturbation methods and is only sketched. Behavior for times such that $u(0) \leq u(s) \leq u_b$ follows by the standard Tikhonov theorem [21] because the critical manifold is normal hyperbolic in that region. The passage through the pitchfork bifurcation for times such that $u_b \leq u(s) \leq u_c$ follows by [22, Theorem 2.2.4] because normal hyperbolicity is lost at the pitchfork and the standard Tikhonov theorem does not apply. Behavior close to the normally hyperbolic stable branches $y = \pm\bar{y}(u)$ for times $s \geq s_4$ follows again by the standard Tikhonov theorem. ■

Remark 6 (Bifurcation delay)**.** *The passage through the pitchfork is characterized by a "bifurcation delay", that is, the system state lies close to the unstable branch of equilibria $y(0)$ for a range of u after the pitchfork bifurcation. This delay is illustrated in Figure 11 right.*

Remark 7 (Guaranteed deadlock breaking)**.** *For any $y_{th} > 0$, the proposed feedback control ensures that deadlock is broken, at least in the generic case $y(0) \neq 0$. On the consensus manifold the disagreement δ is indeed identically zero and, under feedback control, the state converges to $\pm y_{th}\mathbf{1}_N \neq \mathbf{0}$.*

Remark 8 (Informed agents)**.** *For $\boldsymbol{\beta} \neq \mathbf{0}$, we cannot explicitly reduce the closed-loop dynamics* (15) *to two-dimensional dynamics on the consensus manifold. As a result, singular perturbation analysis becomes more involved and will be left for future work. We can however design feedback dynamics for u in the Z_2-symmetric case considered in Theorem 3 and conjecture the behavior of the closed-loop system.*

By Theorem 2, we can reduce the analysis of the closed-loop system with all-to-all graph under Z_2 symmetry, $n_1 = n_2 = n$ informed agents and $n_3 = N - 2n$ uninformed agents to the four-dimensional singularly perturbed dynamics

$$\begin{aligned}
\dot{y}_1 &= -(N-1)y_1 + u\big((n-1)S(y_1) \\
&\qquad + nS(y_2) + n_3 S(y_3)\big) + \beta \\
\dot{y}_2 &= -(N-1)y_2 + u\big(nS(y_1) \\
&\qquad + (n-1)S(y_2) + n_3 S(y_3)\big) - \beta \\
\dot{y}_3 &= -(N-1)y_3 + u\big(nS(y_1) \\
&\qquad + nS(y_2) + (n_3-1)S(y_3)\big) \\
\dot{u} &= \epsilon\left(y_{th}^2 - \left(\frac{1}{N}2n(y_1+y_2) + n_3 y_3\right)^2\right),
\end{aligned}$$

which we write in vector form as

$$\dot{\boldsymbol{y}} = \boldsymbol{f}(\boldsymbol{y}, u), \quad \dot{u} = g(\boldsymbol{y}). \tag{21}$$

By Theorem 3, the critical manifold $\boldsymbol{M}_0 = \{(\boldsymbol{y}, u) : \boldsymbol{f}(\boldsymbol{y}, u) = 0\}$ comprises a single Z_2-symmetric branch $\boldsymbol{y}(u) = \boldsymbol{y}^*(u, \beta)$ for $u \leq u^*$ and three branches $\boldsymbol{y}(u) = \boldsymbol{y}^*(u, \beta)$, $\bar{\boldsymbol{y}}(u, \beta)$, $\gamma\bar{\boldsymbol{y}}(u, \beta)$ for $u > u^*$, where $\boldsymbol{y}^*(u, \beta)$

is again a Z_2-symmetric equilibrium branch and the set $\{\bar{\boldsymbol{y}}(u,\beta), \gamma\bar{\boldsymbol{y}}(u,\beta)\}$ is Z_2-invariant.

We note that $y = 0$ if $\boldsymbol{y} = \boldsymbol{y}^*(u,\beta)$. As in the $\boldsymbol{\beta} = \mathbf{0}$ case the central branch of the critical manifold corresponds to deadlock. The other branches $\bar{\boldsymbol{y}}(u,\beta)$ and $\gamma\bar{\boldsymbol{y}}(u,\beta)$ may or may not correspond to deadlock, depending on the agent spread at those steady states. Because for small β these branches are a small perturbation of the corresponding branches of the critical manifold in the $\boldsymbol{\beta} = \mathbf{0}$ case, stability of each branch is preserved. Despite the larger dimension, we can conjecture that the weakly informed (β small) all-to-all Z_2-symmetric case described by (21) *is qualitatively equivalent to the $\boldsymbol{\beta} = \mathbf{0}$ case sketched in Figure 11.*

B. Control of bifurcation for general network graph

For a general graph we require additional dynamics to allow each agent to estimate the network average opinion y, in order to implement feedback dynamics of the form (15). In [23] dynamics were presented that allow a group of agents to reach dynamic consensus by averaging a time-varying signal. We implement these dynamics to design feedback dynamics as

$$\begin{aligned}
\dot{\boldsymbol{x}} &= -D\boldsymbol{x} + \mathrm{diag}(\boldsymbol{u})AS(\boldsymbol{x}) \\
\dot{\hat{\boldsymbol{y}}} &= -L\hat{\boldsymbol{y}} + \dot{\boldsymbol{x}} \\
\dot{\boldsymbol{u}} &= \epsilon\left(y_{th}^2\mathbf{1}_N - \mathrm{diag}(\hat{\boldsymbol{y}})\hat{\boldsymbol{y}}\right),
\end{aligned} \tag{22}$$

where $\hat{y}_i$ is agent i's estimate of the global average, with $\hat{\boldsymbol{y}}(0) = \boldsymbol{x}(0)$, $L = D - A$, and $\mathrm{diag}(\cdot)$ is the diagonal matrix with elements of the vector argument on the diagonal. For a general graph the agents no longer use the same value of the control parameter, i.e., $\boldsymbol{u}$ is an N-dimensional vector.

For a fixed, strongly connected, and balanced graph, $\mathbf{1}_N^T L = \mathbf{0}$. This implies the following conservation property:

$$\frac{d}{ds}\left(\sum_{i=1}^{N}\hat{y}_i\right) = \frac{d}{ds}\left(\sum_{i=1}^{N}\hat{x}_i\right).$$

Thus, consensus over the estimates $\hat{y}_i$ will track the time-varying average $y = \sum_{i=1}^{N}\hat{x}_i$ [23].

We can write the solution $\hat{\boldsymbol{y}}(s)$ of (22) as

$$\hat{\boldsymbol{y}}(s) = e^{-Ls}\boldsymbol{x}(0) + \int_0^s e^{-Ls}\dot{\boldsymbol{x}}(s-\rho)d\rho.$$

For $\boldsymbol{x}(0) = \mathbf{0}$ and as $s \to \infty$ we have

$$\begin{aligned}
\hat{\boldsymbol{y}}(s) &= \frac{1}{N}\mathbf{1}_N\mathbf{1}_N^T\boldsymbol{x}(s) + \sum_{j=2}^{N}\int_0^s e^{-\lambda_j\rho}\boldsymbol{m}_j\boldsymbol{m}_j^T\dot{\boldsymbol{x}}(s-\rho)\ d\rho \\
&= \frac{1}{N}\mathbf{1}_N\mathbf{1}_N^T\boldsymbol{x}(s) + \boldsymbol{\xi},
\end{aligned}$$

where λ_j and $\boldsymbol{m}_j$ are the $N-1$ non-zero eigenvalues and corresponding eigenvectors of L. Here $\boldsymbol{\xi} = y\mathbf{1}_N - \hat{\boldsymbol{y}}$ is the vector of estimate errors, and these errors can be bounded as a function of the eigenstructure of L. For example, better connected nodes will have larger eigenvalues and lower bounds on their error.

Figure 12 shows simulation results for the dynamics (22) given the five-agent graph shown at the top and $y_{th} = 2$. The top plot shows the opinion of each agent x_i and the average opinion y as a function of time s. It can be seen that the group transitions from deadlock to a collective decision for the alternative B at around $s = 10$ with y going to $-y_{th}$. Agent 5, the least connected node, is last to join the consensus decision.

The middle plot shows each estimate $\hat{y}_i$ versus its control parameter u_i as well as average opinion y versus $\frac{1}{N}\sum_{i=1}^{N} u_i$. These curves are superimposed on the pitchfork associated with the dynamics with $u_i = u$ for all i. The bifurcation delay discussed in Remark 6 is noticeable – the transition to the lower branch solution occurs well after the bifurcation point $u^* = 1$ is reached. The bottom plot shows the components ξ_i of the error vector as a function of time s. The errors converge to zero early on, increase during the transition away from deadlock and then converge again to zero. During the transition Node 5 experiences the largest increase in error.

VII. Conclusion

We have defined an agent-based model that describes distributed dynamics for collective decision-making between alternatives in a multi-agent network. The agent-based dynamics are purposefully designed to exhibit a pitchfork bifurcation so that the mechanisms of collective animal behavior can be formally translated into bio-inspired control design for multi-agent decision-making. Under some symmetry assumptions, we have used this framework to prove agent-based dynamics that inherit the value sensitivity and robust and adaptive features of honeybee nest site selection. The sensitivity of outcomes to model parameters and heterogeneity have been investigated, and slow feedback dynamics have been designed for the bifurcation parameter to enhance control of network decision-making. The framework will be used for control inspired by high performing decision-making of schooling fish and other animal groups. Future work will also make use of singularity theory to address larger classes of network graphs and network heterogeneities.

References

[1] T. D. Seeley and S. C. Buhrman. Nest-site selection in honey bees: how well do swarms implement the "best-of-N" decision rule? *Behavioral Ecology and Sociobiology*, 49:416–427, 2001.

[2] I. D. Couzin, C. C. Ioannou, G. Demirel, T. Gross, C. J. Torney, A. Hartnett, L. Conradt, S. A. Levin, and N. E. Leonard. Uninformed individuals promote democratic consensus in animal groups. *Science*, 334(6062):1578–1580, 2011.

[3] C. Eikenaar, T. Klinner, L. Szostek, and F. Bairlein. Migratory restlessness in captive individuals predicts actual departure in the wild. *Biology Letters*, 10(4), 2014.

[4] J. K. Parrish and L. Edelstein-Keshet. Complexity, pattern, and evolutionary trade-offs in animal aggregation. *Science*, 284(5411):99–101, 1999.

[5] J. Krause and G. D. Ruxton. *Living in Groups*. Oxford University Press, 2002.

[6] D. J. T. Sumpter. *Collective Animal Behavior*. Princeton University Press, 2010.

[7] N. E. Leonard. Multi-agent system dynamics: Bifurcation and behavior of animal groups. *IFAC Ann. Revs. Control*, 38(2):171–183, 2014.

[8] M. Golubitsky and D. G. Schaeffer. *Singularities and Groups in Bifurcation Theory*, volume 51 of *Applied Mathematical Sciences*. Springer-Verlag, New York, NY, 1985.

[9] A. Franci and R. Sepulchre. Realization of nonlinear behaviors from organizing centers. In *IEEE Conference on Decision and Control*, pages 56–61, Los Angeles, CA, December 2014.

[10] F. Castaños and A. Franci. Implementing robust neuromodulation in neuromorphic circuits. *Neurocomputing*, 233:3–13, 2017.

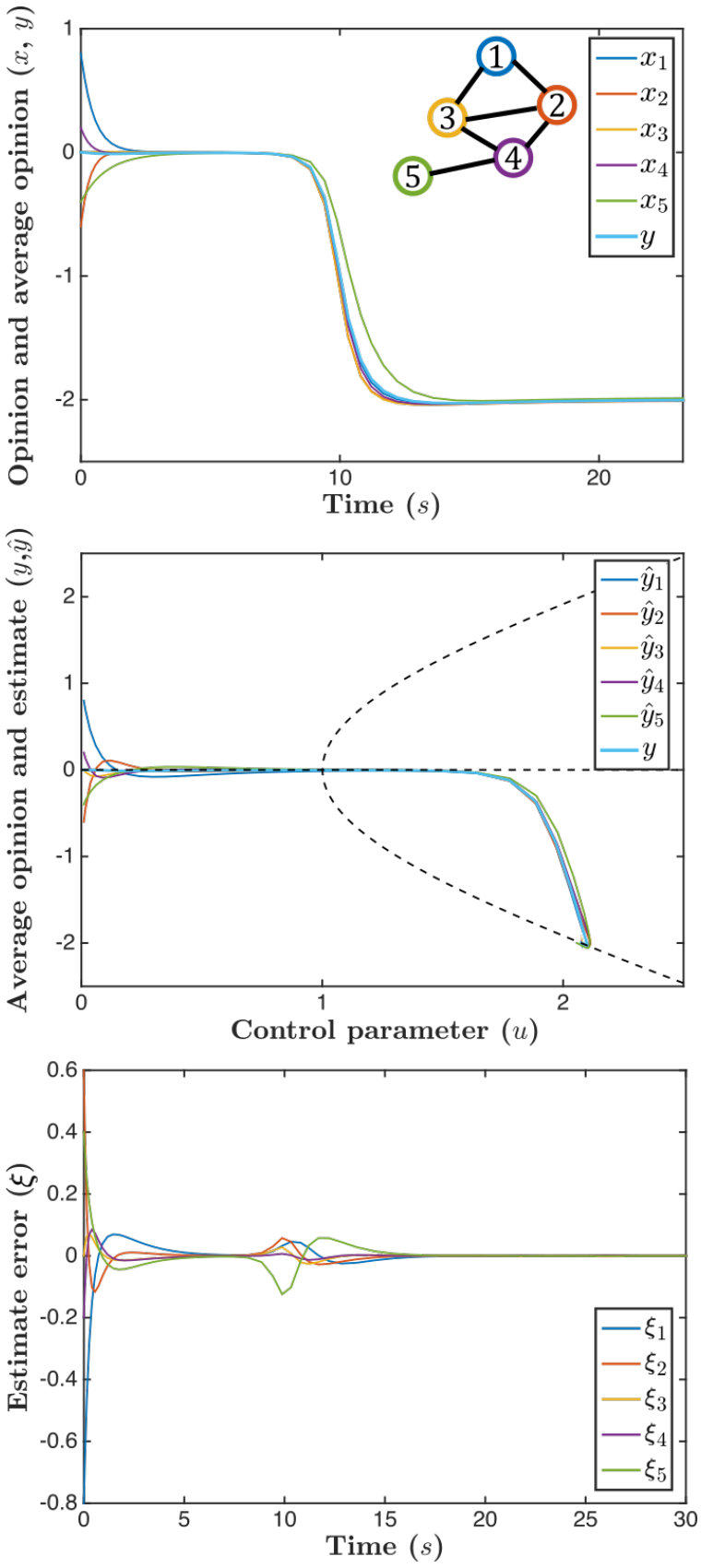

Fig. 12. Simulations of dynamics (22) for the 5-agent graph shown.

[11] T. D. Seeley, P. K. Visscher, T. Schlegel, P. M. Hogan, N. R. Franks, and J. A. R. Marshall. Stop signals provide cross inhibition in collective decision-making by honeybee swarms. *Science*, 335(6064):108–111, 2012.

[12] D. Pais, P. M. Hogan, T. Schlegel, N. R. Franks, N. E. Leonard, and J. A. R. Marshall. A mechanism for value-sensitive decision-making. *PloS ONE*, 8(9):e73216, 2013.

[13] A. Reina, G. Valentini, C. Fernández-Oto, M. Dorigo, and V. Trianni. A design pattern for decentralised decision making. *PLoS ONE*, 10(10):e0140950, 2015.

[14] E. H. Abed and J.-H. Fu. Local feedback stabilization and bifurcation control, Part I: Hopf bifurcations. *Syst. Control Lett.*, 7:11–17, 1986.

[15] G. Chen, J. L. Moiola, and H. O. Wang. Bifurcation control: Theories, methods, and applications. *Int. J. Bifur. Chaos*, 10(3):511–548, 2000.

[16] A. J. Krener, W. Kang, and D. E. Chang. Control bifurcations. *IEEE Transactions on Automatic Control*, 49(8):1231–1246, 2004.

[17] J. J. Hopfield. Neural networks and physical systems with emergent collective computational abilities. *Proceedings of the National Academy of Sciences*, 79(8):2554–2558, 1982.

[18] J. J. Hopfield. Neurons with graded response have collective computational properties like those of two-state neurons. *Proceedings of the National Academy of Sciences*, 81(10):3088–3092, 1984.

[19] J. Guckenheimer and P. Holmes. *Nonlinear Oscillations, Dynamical Systems, and Bifurcations of Vector Fields*, volume 42 of *Applied Mathematical Sciences*. Springer, New-York, 7th edition, 2002.

[20] W. Govaerts and Y .A. Kuznetsov. MATCONT and CL MATCONT: Continuation toolboxes in MATLAB. https://sourceforge.net/projects/matcont/, August 2015.

[21] H. K. Khalil. *Nonlinear systems*. Prentice Hall, third edition, 2002.

[22] N. Berglund and B. Gentz. *Noise-induced phenomena in slow-fast dynamical systems*. Springer-Verlag, London, 2006.

[23] D. Spanos, R. Olfati-Saber, and R.M. Murray. Dynamic consensus for mobile networks. In *Proc. 16th IFAC World Congress*, pages 1–6, Prague, 2005.